Symmetry and phase transitions in Langmuir monolayers: The Landau theory

V.M. Kaganer and E.B. Loginov
Institute of Crystallography, Russian Academy of Sciences, Leninskii pr.59, 117333 Moscow, Russia
(Received 7 April 1994)

Condensed phases of Langmuir monolayers are treated in the framework of the Landau theory of phase transitions as a result of successive ordering of the hexatic phase. All types of ordering allowed by symmetry and the couplings between them are described. The phase diagrams and x-ray structural data on monolayers of various long-chain amphiphilic molecules can be explained by using three coupled order parameters. One of the parameters governs the collective tilt of the molecules, while the other two describe one-dimensional "weak crystallization" involving herringbone ordering of the molecular backbone planes along the bond direction and normal to it. Possible manifestations of other order parameters are discussed.

PACS number(s): 61.50.Ks, 68.10.−m, 68.35.Rh

I. INTRODUCTION

A. Phases of Langmuir monolayers

Transitions between condensed phases of Langmuir monolayers were first observed as kinks in the surface pressure-area isotherms more than fifty years ago [1]. Systematic measurements by Stenhagen [2,3] and Lundquist [4,5] gave rise to the phase diagrams which have been modified since then only in their fine structure [6]. Monolayers of different amphiphiles possess very similar phase diagrams. Although the measurements on any substance are performed in a limited temperature range, a generalized phase diagram [6] can be compiled from isotherm studies of amphiphiles with different chain lengths by matching up regions of the same shape with regular shifts of the temperature axis [7]. Two experimental techniques, Brewster angle microscopy [8] and polarized fluorescence microscopy [9], were used to determine the phase diagram of fatty acid monolayers reproduced in Fig. 1(a). It contains a new transition line which was not apparent in isotherm measurements. We follow the Harkins-Stenhagen notation [1–3] of the phases, and denote by Ov the phase found in [8].

Recent x-ray diffraction experiments [10–19] have shown that all kinks in the isotherms observed by Stenhagen and Lundquist are due to structural phase transitions and all regions of Fig. 1(a) have different structures. In the high-pressure phases LS, S, and CS the molecules are not tilted on average. The LS phase possesses one broad first-order diffraction peak. The correlation length determined from the full width at half maximum of the peak varies from about 20 intermolecular distances at high temperatures [17] to 5–7 intermolecular distances near the LS-S transition [14]. Monodomain samples are not available for x-ray studies and the single peak of the "powder" sample is interpreted as the triply degenerate peak of a hexatic phase. The hexatic order in the LS phase was not observed directly. The sixfold axes of the domains of the tilted phase L_2 in coexistence with the higher-temperature two-dimensional liquid phase L_1 were revealed by fluorescence microscopy [20]. At the LS-S transition the single peak of the LS-phase splits into two, one doubly degenerate and one nondegenerate, both with correlation lengths of about 30 intermolecular distances. This orthorhombic distortion can be interpreted as due to the ordering of the short axes (backbone planes) of the molecules. Although this interpretation is not confirmed by experiment since no higher-order peaks were observed, herringbone order is expected in analogy with smectic-E liquid crystals [21] and bulk alkanes [22]. The theory presented below confirms this suggestion. The other possible variant, nematiclike ordering of the backbone planes parallel to each other, contradicts the structural data ([23]; see also Sec. II A 2). The CS phase gives the resolution-limited peaks of a two-dimensional solid. The transitions LS-S and S-CS are first order, as was first determined by isotherm measurements and then confirmed with x-ray diffraction.

As the surface pressure is lowered, transitions occur to the phases showing collective tilt of the molecules. The tilting transitions CS-L_2'', S-L_2', LS-L_2, and LS-Ov are found to be continuous. The phase L_2'' possesses the resolution-limited peaks of a two-dimensional solid whereas L_2', L_2, and Ov are mesophases. The molecules tilt in the direction toward the nearest neighbor in L_2 and L_2'' phases and toward the next-nearest neighbor in L_2' and Ov phases, the swiveling transitions being obviously of the first order. The L_2-Ov transition is much weaker than the L_2-L_2' transition and was not revealed by isotherm measurements. It was detected recently by Brewster angle microscopy [8] and polarized fluorescence microscopy [9]. The tilt direction in the Ov phase was determined by x-ray diffraction [19]. In the x-ray diffraction experiments, isotherm scans over the phase sequence S-L_2'-L_2 revealed drastic changes in the correlation lengths at the L_2'-L_2 transition [14]. The correlation lengths for the two peaks in the L_2' phase differ only slightly from those in the S phase, being about 30 intermolecular distances. In the L_2 phase, the nondegenerate peak shows a correlation length of about 60 intermolecular distances whereas for the doubly degenerate one the correlation

length is about four times smaller. Essential differences in the correlation lengths of two peaks were found also for the monolayers of the longer-chain fatty acids in an uncompressed state [24,25]. These differences find a natural explanation in the theory presented below.

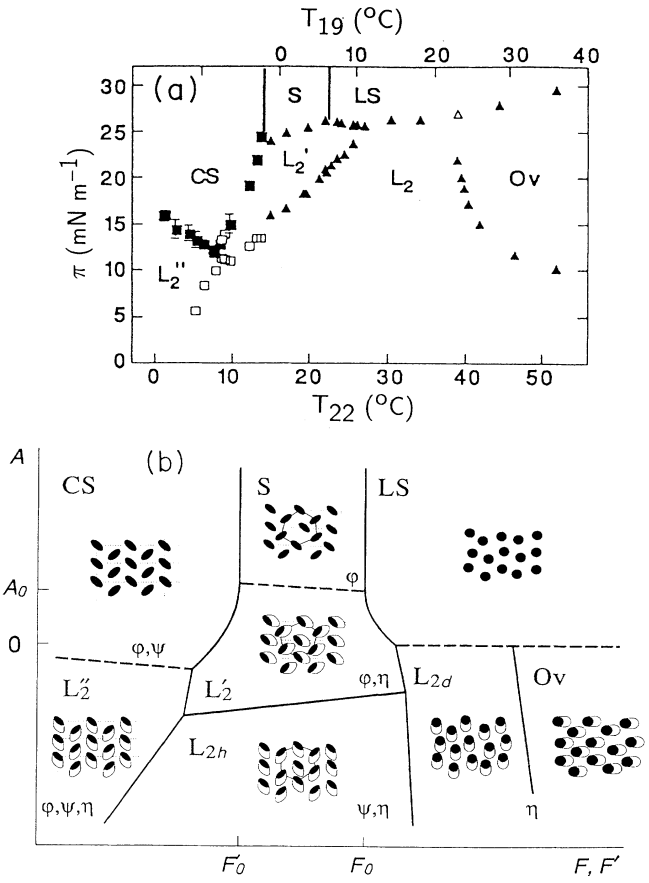

FIG. 1. (a) Experimental phase diagram for fatty acid monolayers from Schwartz and Knobler [9]. Squares refer to observations of behenic (C_{22}) acid, while triangles refer to arachidic (C_{19}) acid (adjusted to overlay the behenic acid data by adding 10 °C to the temperature). The open symbols refer to transitions determined only by isotherm features; others are from polarized fluorescence microscopy data. To the original figure we have added, following Ref. [19], the label Ov for the Overbeck and Möbius phase [8], and an axis along the top of the figure to indicate the temperatures for C_{19} acid. Additionally, the phase S and solid lines for its boundaries are added according to Refs. [2,3], while the Brewster angle microscopy data is omitted. (b) Theoretical phase diagram. F, F' are the temperaturelike variables and A is the surface pressure-like one. Solid lines denote the first-order transitions, dashed lines indicate the second-order ones. The phases presented are the hexatic phase LS, tilted hexatic phases L_{2d} and Ov, one-dimensional (1D) crystal phases S, L_2', and L_{2h}, and herringbone-ordered 2D crystal phases CS and L_2''. The tilted hexatic phases L_{2d} and Ov differ in direction of tilt with respect to the bonds, while the phases L_2' and L_{2h} differ in both direction of crystallization wave and direction of tilt with respect to bonds. Greek letters indicate nonzero order parameters in each phase.

B. The Landau theory of phase transitions

In the theory of phase transitions proposed by Landau [26,27], one of the basic ideas is to expand the free energy as a power series in an order parameter related to the changes of symmetry at the structural phase transition. In its rigorous formulation, this idea can be used to predict the continuous (second-order) phase transformations which can occur for a given symmetry of the more symmetrical phase. A number of approximations, verified on different systems, have been proposed to extend its applicability (see, e.g., [28] for a review). First-order transitions are widely treated using Landau free energy expansions, with reasonable accuracy provided the discontinuities at the transitions are small. The phase transitions in liquid crystals are an appropriate example. Successive phase transitions can also be considered, with reduced accuracy, using free energy expansions based on the symmetry of the most symmetrical phase.

Landau specifically considered the crystallization phase transition, for which he took the amplitude of the density wave as the order parameter [27]. He showed that the crystallization transition is first order. His idea was developed further in the "weak crystallization" theory which considers, in the framework of the Landau free energy expansion, the formation of different crystalline structures (see, e.g., [29] for a recent review). This theory assumes that the wave vectors participating in crystallization have equal lengths and the discontinuities at the transition are small. Both requirements are met, for example, at the nematic-smectic phase transition (one-dimensional crystallization over a density wave) and for formation of the blue phase of liquid crystals (three-dimensional crystallization over a tensor quantity). Waves of vector or tensor components can lead to second-order transitions for symmetry reasons. Antiferroelectric ordering of transverse dipoles is an example.

The aim of the present work is to consider, in the framework of the Landau theory, the whole set of transitions between condensed phases of Langmuir monolayers. Hexatic symmetry is assumed for the most symmetrical condensed phase LS. A free energy expansion based on hexatic symmetry is applied to the whole phase diagram of Fig. 1(a), since all observed transitions occur over a temperature range of less than 20 °C. Both hexatic-to-hexatic and crystallization transitions are considered.

C. Summary of the results

1. *Types of ordering*

All types of ordering of the hexatic phase allowed by its symmetry are listed in Fig. 2. Of these eight, the top four [Figs. 2(a)–(d)] give rise to phases preserving the continuous translational order of the hexatic phase. Although they are less symmetrical than the initial hexatic phase, they are still called "hexatic" phases in order to emphasize their continuous translational order. Here we follow Refs. [30,31] where the "tilted hexatic" phase was considered. The phase 2(a) is characterized by an order

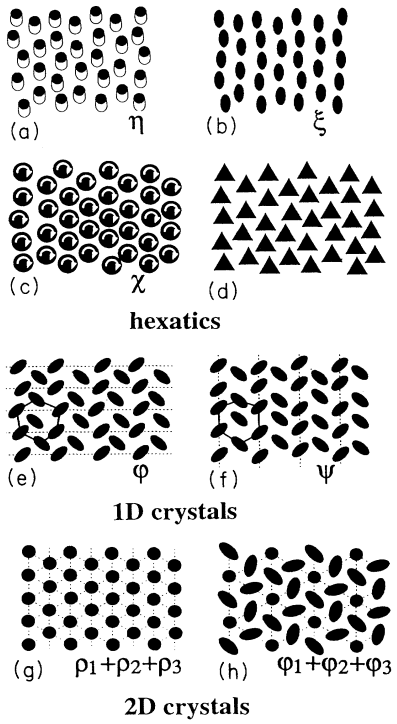

FIG. 2. All possible ways for ordering of the two-dimensional hexatic phase: (a)–(d) the phases possessing continuous translational order (hexatic phases); (e), (f) phases with one crystallization wave (one-dimensional crystals); (g), (h) phases with three crystallization waves (two-dimensional crystals). Broken lines indicate periodicity. Greek letters refer to notation of the order parameters in the paper.

parameter which is a two-dimensional vector lying in the plane of the monolayer. One suitable implementation is the projection of the vector, describing collective tilt, directed along the long axes of the molecules. Another is the vector oriented parallel to the molecular heads. The symmetries of both these implementations are the same, and the presence of one induces the other. We treat this order in terms of collective tilt of the molecules, which has been observed in Langmuir monolayers. There are two preferred directions of tilt, both along symmetry planes of the hexatic phase. In the first, the tilt is towards a nearest neighbor (NN) molecule along the bonds, as shown in the figure. In the second, the tilt is towards a next-nearest neighbor (NNN), normal to the bonds. An intermediate tilt direction is also possible.

Figure 2(b) represents the ordering of the short axes of the molecules parallel to each other. For Langmuir monolayers, the term "short axes" is used interchangeably with "backbone planes," "zigzag planes," or "planes of the carbon skeleton of the molecules." The backbone planes can be oriented to the nearest neighbor (as shown on the figure), to the next-nearest neighbor, or in an intermediate direction. Figure 2(c) demonstrates the phase of chiral molecules which is derived from the hexatic by preserving the sixfold symmetry and losing the symmetry planes. Examples of chiral amphiphiles are fluorinated fatty acids [32–34]. At the transition to the phase of Fig. 2(d) the sixfold symmetry of the hexatic phase is reduced to threefold symmetry. Two variants of this phase are possible, depending on the symmetry plane preserved. The transitions to the phases Fig. 2(c) and Fig. 2(d) are not found in Langmuir monolayers and we will not consider them further. The transition from the hexatic to the phase of Fig. 2(b) is first order, whereas the phases of Figs. 2(a), 2(c), and 2(d) can appear continuously (Sec. II A).

The two-dimensional hexatic phase can crystallize in two ways, giving rise either to one-dimensional crystalline order as in Figs. 2(e) and 2(f), or to two-dimensional crystals as in Figs. 2(g) and 2(h). The phase of Fig. 2(g) is appropriate when the order parameter is the amplitude of the density wave. The symmetry of the hexatic phase requires three waves with equal amplitudes, directed at 120° to each other, giving rise to a hexagonal crystal. The transition from hexatic phase to hexagonal crystal must be first order, because the density is a scalar quantity which does not change sign on reflection. The transverse component of a vector or tensor provides an order parameter which changes sign on reflection in the symmetry plane containing the wave vector. Figures 2(e), 2(f), and 2(h) demonstrate crystallization over these order parameters. Both one-dimensional crystallization due to a single wave, Fig. 2(e) and Fig. 2(f), and two-dimensional crystallization due to three waves with equal amplitudes, Fig. 2(h), are possible, and all transitions can be continuous. The order within the rows of molecules in phases Fig. 2(e) and Fig. 2(f) is liquidlike. The phases Fig. 2(e) and Fig. 2(f) differ from each other in the direction of the wave vector of the crystallization wave to the nearest neighbor of Fig. 2(f) or to the next-nearest neighbor of Fig. 2(g). The antiferroelectric type of ordering of a vector and the herringbone type of ordering of a tensor (the latter is presented on the figure) are both described by these waves and, moreover, always accompany each other (see Sec. II B 2). In Langmuir monolayers, herringbone ordering is expected by analogy with smectic-E phases [21] and bulk alkanes [22], so that we discuss these phases in terms of herringbone order.

Although the phases of Fig. 2(e) and Fig. 2(f) are very similar, their diffraction patterns differ. In Fig. 2(e), the bonds do not lie in the crystalline rows. This gives broad first-order diffraction peaks, reflecting the liquid-like order. In contrast, the diffraction pattern of the phase Fig. 2(f) shows one narrow peak due to diffraction from the crystalline rows, while the doubly degenerate peak caused by the short-range translational order within the rows is broad. Comparing these results with the experimental data on the diffraction peak widths, we can attribute the phase of Fig. 2(e) to the phases S and L_2' of Langmuir monolayers possessing first-order peaks of approximately equal widths whereas Fig. 2(f) corresponds to the phase L_2 with considerably different peak widths. The phase Fig. 2(h) is a two-dimensional crystal with four molecules per unit cell. It has not been found in Langmuir monolayers.

2. Theoretical phase diagram

The theoretical phase diagram of the present paper, Fig. 1(b), is constructed to satisfy simultaneously the symmetry requirements of the Landau free energy expansion and the experimental data, both thermodynamic and structural. The nomenclature of the observed phases is preserved; the phase L_2 is subdivided, for symmetry reasons, into two phases, L_{2d} and L_{2h}. All features of the theoretical phase diagram are derived from the unique free energy expansion invariant with respect to the hexatic symmetry of the most symmetrical phase, LS. The ordering of the backbone planes of the molecules is considered to occur with decreasing temperature, whereas the tilting transitions are due to decreasing surface pressure, as found in experiments.

The transitions LS-L_{2d} and LS-Ov are transitions from the hexatic to "tilted hexatic" phases possessing different tilt directions. Both tilted phases have continuous translational symmetry. For the transition LS-S, revealed experimentally by an orthorhombic distortion, symmetry arguments allow two possibilities, nematiclike ordering of the backbone planes, Fig. 2(b), and one-dimensional crystallization, Fig. 2(e). The phase of Fig. 2(f) can be ruled out since the first-order diffraction peaks remain broad in phase S. Nematiclike ordering provides a suitable description of the corresponding part of the phase diagram with phases LS, S, L_2', and L_{2d}, but does not fit the structural data ([23]; see also Sec. II A 2). In brief, it is observed experimentally that the tilt in phase L_{2d} induces weak (proportional to the square of the tilt angle) nematic order with the backbone planes oriented in the same direction as the tilt, i.e., toward the nearest neighbor. The spontaneous ordering at the LS-S transition also orients the backbone planes in the NN direction, as shown in Fig. 2(b). Then the tilt at the S-L_2' transition is expected to be in the same direction, contrary to the observations of NNN tilt in the phase L_2'. Hence the one-dimensional crystal phase of Fig. 2(e) remains the only candidate for the symmetry of the S phase. Its coupling with the tilt satisfies both the thermodynamic and the structural data for the phases LS, S, L_2', and L_{2d}, and transitions between them (Sec. II C).

The transition S-CS is due to the appearance, at some temperature below the LS-S transition, of the crystallization wave shown in Fig. 2(f). The phase CS, which possesses two crystallization waves with orthogonal wave vectors, is a two-dimensional crystal. As the surface pressure is lowered at a temperature corresponding to the S phase, the increasing tilt angle acts similarly to the decreasing temperature, switching on the crystallization wave of Fig. 2(f) at the L_2'-L_{2h} transition. The tilt direction changes at the transition, which cause the S-phase order parameter to disappear. The phase L_{2h} also possesses one-dimensional crystalline order, differing from that of the L_2' phase in its directions of tilt and crystallization.

The transition CS-L_2'' is the tilting transition in a two-dimensional crystal. In the framework of the unified free energy expansion invariant with respect to symmetry of the hexatic phase, the lines of the tilting transitions LS-Ov, LS-L_{2d}, S-L_2', and CS-L_2'' are almost parallel and shift with respect to each other when crossed by the lines of the first-order transitions LS-S and S-CS. The positions of the phase transition lines are discussed in Sec. III. The lowest-order terms of the free energy expansion are considered to be temperature and surface pressure dependent, whereas all other coefficients are taken to be constants, as in the standard approach to Landau theory. This assumption is valid in the vicinity of a transition line, but cannot be applied for quantitative analysis over a finite range of the external variables. Variations of the higher-order coefficients can continuously distort the phase diagram. However, this does not change the conclusions about the topology of the phase diagram or the structure of the phases.

The present theory employs one and the same free energy expansion for a whole range of temperatures and surface pressures. In this way, the phase diagram containing seven observed phases is explained by the coupling of just three order parameters. There remain slight ambiguities related to the presence of first-order transitions. In particular, comparison of the diffraction data with bulk crystal structures might suggest that the backbone planes in the phase L_{2h} are parallel to each other, without herringbone order. In this case the phases L_{2d} and L_{2h} would possess the same symmetry, thus explaining the absence of the L_{2d}-L_{2h} transition from the experimental phase diagram. An adequate theoretical description here of the structural data requires higher-order terms, making the results much less definite (see Sec. IV). To avoid these difficulties, we limit ourselves to the phase diagram of Fig. 1(b) which involves only the lowest-order terms in the free energy expansion over the present order parameters.

II. PHASE TRANSITIONS FROM THE HEXATIC PHASE

A. Hexatic-to-hexatic transitions

1. Tilting

The most symmetrical phase of the present theory, the hexatic phase, is assumed to possess continuous translational order, as in a liquid, and discrete orientational order of the point symmetry group C_{6v} generated by a sixfold symmetry axis and two orthogonal symmetry planes normal to the plane of the monolayer. In Sec. II A we consider transitions decreasing orientational symmetry and preserving continuous translations. The resulting phases are called "hexatic" in order to stress that these phases remain anisotropic liquids, as the initial hexatic phase. Let us consider first the "tilted hexatic" phase appearing due to the collective tilt of the molecules.

Introducing the unit vector $\boldsymbol{n}$ along the mean direction of the long axes of the molecules, one can consider its components n_x, n_y in the plane of the monolayer to be a two-dimensional order parameter describing the collective tilt of the molecules. It is convenient to convert to polar coordinates η, β:

$$n_x = \eta\cos\beta, \quad n_y = \eta\sin\beta. \tag{1}$$

Here β is the azimuthal angle of the collective tilt and $\eta = \sin\theta$, where θ is the tilt angle. One has $\eta = 0$ in the phase of untilted molecules and $\eta \neq 0$ for collective tilt. The sixfold rotation transforms the azimuthal angle according to $\beta \to \beta + \pi/3$, and the reflections in the orthogonal symmetry planes give rise to $\beta \to -\beta$ and $\beta \to \pi - \beta$. The expansion of the free energy invariant with respect to these transformations is

$$\Phi_\eta = A\eta^2 + B\eta^4 - D\eta^6\cos 6\beta + E\eta^{12}\cos 12\beta. \tag{2}$$

The first two terms in Eq. (2) are sufficient to describe the second-order phase transition at $A = 0$, provided $B > 0$: for $A > 0$, the minimum of the free energy is achieved at $\eta = 0$; as A changes sign, the minimum continuously shifts to $\eta^2 = -A/2B$.

The last two terms in Eq. (2), small in comparison with the first ones, are the lowest-order terms depending on the tilt azimuth β. They are included in the free energy expansion (2) owing to degeneracy of the fourth-order term with respect to β. Polar coordinates (1) provide a compact notation for the anisotropic terms. They can be expanded if necessary in terms of the components n_x, n_y of the order parameter by expressing $\cos 6\beta$ and $\cos 12\beta$ as mixed homogeneous polynomials in $\sin\beta$ and $\cos\beta$. For example, the term $\eta^6\cos 6\beta$ is equal to $(n_x^2 - n_y^2)[(n_x^2 - n_y^2)^2 - 12n_x^2n_y^2]$. The polar coordinate notation makes the sixfold symmetry of the expression much more evident. For $D > 0$, minimization of Φ_η over β gives $\beta = \pi m/3$ (m is integer), i.e., NN tilt occurs. If $D < 0$, the minimum is achieved at $\beta = \pi/6 + \pi m/3$, i.e., for NNN tilt. As D varies from positive to negative values, the last term in Eq. (2) becomes comparable with the lower-order one. If $E < 0$, the first-order transition NN $\to$ NNN occurs at $D = 0$. If $E > 0$, the tilt azimuth takes on intermediate values $0 < \beta < \pi/3$ (I phase) over the range $|D| < 4E\eta^6$ with second-order phase transitions NN $\to$ I $\to$ NNN at each end. The transitions between tilted phases were analyzed in detail by Selinger and Nelson [35,36] taking fluctuations into account. It was shown that, over a certain range of the coefficients, both D and E tend to zero on renormalization to macroscopic scale. This introduces an "unlocked tilted phase" to the phase diagram. The two tilted hexatic phases observed in fatty acid monolayers, labeled L_2 and Ov in Fig. 1(a), possess NN and NNN tilt, respectively, and the free energy expansion (2) with $E < 0$ describes both of them, giving the L_2 phase for $D > 0$ and the Ov phase for $D < 0$.

2. *Ordering of the backbone planes*

Consider now the ordering of the backbone planes (short axes) of the molecules, as shown in Fig. 2(b). When the molecules order in this way, the first-order diffraction peak of the hexatic phase splits to two peaks, reflecting "long" and "short" distances between neighbor molecules. In describing x-ray diffraction experiments, the splitting is usually referred to as a distortion of the unit cell. Although the term "unit cell" cannot be rigorously applied to noncrystalline phases, it provides a clear description of the diffraction data. For example, one can characterize the phase of Fig. 2(b) as an expansion of the unit cell in the NN direction. This terminology does not cause any misunderstanding and we shall use it further on.

More rigorously, the phase of Fig. 2(b) is due to the in-plane nematic ordering of the backbone planes. The order is described by the director $\boldsymbol{N}$ — the vector in the plane of the monolayer parallel to the backbone plane orientation, $\boldsymbol{N}$ and $-\boldsymbol{N}$ being equivalent. The last statement distinguishes the director from the tilt vector $\boldsymbol{n}$ considered above. Following the standard description of the nematic phases [37], one can introduce the nematic order parameter $\hat{Q}$ — a symmetrical 2D traceless tensor with components $Q_{ij} = N_iN_j - \frac{1}{2}\delta_{ij}$ $(i, j = 1, 2)$. This tensor plays the same role here as the strain tensor in crystalline phases, thus justifying the terminology discussed above. The two independent components of the traceless 2D tensor $\hat{Q}$ can be represented in polar coordinates:

$$Q_{xx} - Q_{yy} = \xi\cos\alpha, \quad 2Q_{xy} = \xi\sin\alpha. \tag{3}$$

The case $\xi = 0$ corresponds to the hexagonal symmetry of the LS phase whereas $\xi \neq 0$ gives phases with distorted unit cells. One has $\alpha = 0$ when the nematic director points along the bonds (or the unit cell stretches to the NN) and $\alpha = \pi$ when the director is perpendicular to the bonds (or the unit cell stretches to the NNN). On rotation of the monolayer through the angle $\pi/3$ the components (3) of the second-rank tensor are transformed by two rotation matrices according to $\alpha \to \alpha + 2\pi/3$. The free energy expansion invariant with respect to the sixfold rotation and the reflections in symmetry planes (which transform $\alpha \to -\alpha$) is

$$\Phi_\xi = C\xi^2 - K\xi^3\cos 3\alpha + L\xi^4. \tag{4}$$

When the third-order term is simplified by expanding $\cos 3\alpha$ as a homogeneous polynomial in powers of $\sin\alpha$ and $\cos\alpha$, it becomes $(Q_{xx} - Q_{yy})[(Q_{xx} - Q_{yy})^2 - 12Q_{xy}^2]$. Substitution of the tensor components Q_{ij} by a diad n_in_j reduces this term to the term $\eta^6\cos 6\beta$ in Eq. (6).

The presence of the third-order term in Eq. (4) leads to a first-order phase transition of the order parameter ξ [38]: the free energy (4) has two local minima, $\xi = 0$ and $\xi \neq 0$, and as F changes a transition occurs when the minimum at $\xi \neq 0$ becomes deeper. The minimum with respect to the angle α occurs at $\alpha = 0$ for $K > 0$ and at $\alpha = \pi$ for $K < 0$ (equivalent angles differing from the stated ones by $2\pi m/3$ are not mentioned hereafter for the sake of simplicity). More accurately, taking into account the α-dependent term of next highest order $K'\xi^6\cos 6\alpha$ in the free energy expansion, there is a first-order transition from $\alpha = 0$ to $\alpha = \pi$ when $K' < 0$ and K changes from positive to negative values. Both phases possess orthorhombic symmetry, and the unit cell either stretches or shrinks, respectively, in the NN direction. On the other hand, if $K' > 0$, these phases are linked by second-order phase transitions at $K = \pm 4K'\xi^3$. In the

intermediate phase α varies continuously, and the unit cell has monoclinic symmetry.

The coupling between ξ and the order parameter η responsible for the tilt is due to the lowest-order term

$$\Phi_{\xi\eta} = -V\xi\eta^2 \cos(\alpha - 2\beta), \tag{5}$$

which is invariant with respect to sixfold rotation (transforming $\alpha \to \alpha + 2\pi/3, \beta \to \beta + \pi/3$) and reflection ($\alpha \to -\alpha, \beta \to -\beta$). At temperatures above the transition over ξ the tilt induces distortions: the minimum of the first term of Eq. (4) together with Eq. (5) gives $\xi \sim \eta^2$. The sign in Eq. (5) is chosen so that at $V > 0$ the NN tilt with $\beta = 0$ causes the unit cell to stretch along the bonds, $\alpha = 0$, as is observed at the LS-L_2 transition in fatty acids.

The manifestation of the LS-S transition in the diffraction experiments is orthorhombic distortion with the stretch of the cell to the NN (i.e., $\alpha = 0$). However, the description of this transition as a spontaneous ordering of the backbone planes with the free energy (4) is not consistent with the structural data [23]. If the phase S is formed by the transition over ξ and the observed distortion direction $\alpha = 0$ is due to a minimum of Eq. (4) with $K > 0$, then the tilt direction at the transition S-L_2' given by Eq. (5) is $\beta = 0$, since $V > 0$ as was derived above from the direction of the induced distortions at the LS-L_2 transition. However, the observed tilt in the L_2' phase is in the NNN direction ($\beta = \pi/2$). The phase diagram of fatty alcohols and corresponding diffraction data [18] also cannot be explained with a transition over ξ between LS and S phases [23]. Fatty alcohols possess only NNN tilt, so that the whole region of L_2 and L_2' phases is revealed in the diffraction experiment as a single phase. (Recently, Lawrie and Barnes [39] found, by means of isotherm measurements, a phase transition line inside the tilted phase of a fatty alcohol. It is treated similarly to the transition inside the L_2' phase of fatty acids [6], also found by isotherm studies and not revealed in diffraction experiments.) The tilting transition from the LS phase can be described by Eq. (2) with $D < 0$, giving $\beta = \pi/2$. The unit cell is observed to stretch in the tilt direction ($\alpha = \pi$), which is described by Eq. (5) with $V > 0$. At the LS-S transition, the unit cell stretches to the NN ($\alpha = 0$), in the same direction as in the fatty acids. In this case the coupling term (5) with $V > 0$ as already determined requires NN tilt at the tilting transition from the S phase. In contradiction to this, NNN tilt is observed. It is shown below in Sec. II C that the distortion ξ in phase S of both fatty acids and alcohols is induced by the other primary order parameter, describing herringbone ordering of the backbone planes.

3. Chirality

Examples of chiral amphiphiles which form Langmuir monolayers are the fluorinated fatty acids [32–34]. Although the transition shown in Fig. 2(c) from a nonchiral to a chiral phase has not yet been observed, we describe briefly, for the sake of completeness, its main features. The order parameter χ for the chirality phase transition is a pseudoscalar changing sign on reflections and invariant with respect to rotations. The cubic term in the free energy expansion over the powers of χ is forbidden by the reflection symmetry, so that the expansion

$$\Phi_\chi = a\chi^2 + b\chi^4 \tag{6}$$

allows a continuous transition at $a = 0$.

The coupling with the order parameters η and ξ introduced above is due to the terms

$$\Phi_{\chi\eta\xi} = c\chi\eta^6 \sin 6\beta + d\chi\xi^3 \sin 3\alpha. \tag{7}$$

The multipliers of each term of Eq. (7) do not change on 60° rotation whereas on reflection both χ and sine terms change sign, so that the right-hand side of Eq. (7) is invariant with respect to symmetry of the hexatic phase. Equation (7) is linear over χ, and, taking into account the quadratic term of Eq. (6), one finds that the nonzero chirality $\chi = (c/2a)\eta^6 \sin 6\beta + (d/2a)\xi^3 \sin 3\alpha$ is induced by tilt η or distortion ξ, provided that both tilt and distortion occur in a direction intermediate between NN and NNN.

One has to distinguish this case of induced chirality from the transition over χ occurring when the coefficient a in Eq. (6) becomes negative. Induced chirality is a secondary effect when the direction of tilt or distortion varies, and χ-dependent terms can be excluded from the free energy expansion by minimizing first over χ. Our approach here disagrees with that of Selinger *et al.* [40] where the difference between induced and spontaneous chirality was not taken into consideration.

The transition from sixfold to threefold symmetry, Fig. 2(d), is not realized in Langmuir monolayers, but can be expected for monolayers of molecules with threefold symmetry, like NH_3. A single-component order parameter describing the transition changes sign on 60° rotation, so that the cubic term is absent in the free energy expansion and the transition can be continuous. There are two possible transitions, differing in the symmetry plane retained.

The transitions considered above, Figs. 2(a)–2(d), include all different representations of the point symmetry group C_{6v} of the hexatic phase and thus exhaust the list of possible ways of ordering of the hexatic phase preserving continuous translational symmetry.

B. Crystallization transitions

1. Density waves

Crystallization of a liquid or hexatic phase consists in the appearance of periodic spatial variations in the density function. "Weak crystallization" theory assumes that in the Fourier expansion of the density function all essential terms $u_j \exp(i\boldsymbol{k}_j \cdot \boldsymbol{r})$ have equal lengths of the wave vectors [27]. Since the experimentally observed phases possess at least orthorhombic symmetry, we can restrict ourselves to $\boldsymbol{k}$ vectors lying in the symmetry planes. By successive application of sixfold rotation C_6 to a wave vector, six wave vectors $\boldsymbol{k}_{j+1} = C_6\boldsymbol{k}_j$ are seen

to participate in crystallization. The order parameter has six components u_j and, since the density function $\sum_j u_j \exp(i\boldsymbol{k}_j \cdot \boldsymbol{r})$ must always be real, it follows that $u_{j+3} = u_j^*$. It is convenient to designate

$$u_1 = \rho_1 e^{i\gamma_1},\ u_2 = \rho_2 e^{i\gamma_2},\ u_3 = \rho_3 e^{i\gamma_3},$$
$$u_4 = \rho_1 e^{-i\gamma_1}, u_5 = \rho_2 e^{-i\gamma_2}, u_6 = \rho_3 e^{-i\gamma_3}. \quad (8)$$

The only invariant terms in the free energy expansion over the corresponding order parameters u_j are those combinations of the u_j's with $\boldsymbol{k}$ vectors constituting a closed polygon ($\sum_j \boldsymbol{k}_j = 0$). Then the free energy expansion is

$$\Phi_\rho = P(u_1u_4 + u_2u_5 + u_3u_6) + Q(u_1u_3u_5 + u_2u_4u_6) + R(u_1u_4 + u_2u_5 + u_3u_6)^2 + S(u_1^2u_4^2 + u_2^2u_5^2 + u_3^2u_6^2). \quad (9)$$

Taking into account Eq. (8), one reduces Eq. (9) to

$$\Phi_\rho = P\rho^2 + Q\rho_1\rho_2\rho_3\cos(\gamma_1 + \gamma_2 + \gamma_3) + R\rho^4 + S(\rho_1^4 + \rho_2^4 + \rho_3^4), \quad (10)$$

where $\rho^2 = \rho_1^2 + \rho_2^2 + \rho_3^2$. The fourth-order terms must be positive definite, in order to ensure stability of the ordered phase; otherwise, higher-order terms should be included in the expansion. The presence of the cubic term in Eq. (10) means that the transition is first order. Equation (10) can be minimized first over the phases γ_j of the density waves. Negative Q gives $\gamma_1 + \gamma_2 + \gamma_3 = 0$, which leads to the hexagonal crystal structure. For positive Q one has, with $\gamma_1 + \gamma_2 + \gamma_3 = \pi$, a complementary structure with density minima on the sites of the hexagonal lattice, which is unlikely to occur experimentally. Let us now minimize Eq. (10) over ρ^2, keeping the ratios $\mu_j = \rho_j/\rho$ constant. For sufficiently large P, the absolute minimum is the one at $\rho = 0$. As P decreases beyond

$$P = \frac{1}{4}\frac{(Q\mu_1\mu_2\mu_3)^2}{R + S(\mu_1^4 + \mu_2^4 + \mu_3^4)}, \quad (11)$$

the minimum at $\rho \neq 0$ becomes deeper. Then the phase transition is realized for the ratios $\{\mu_j\}$ which maximize the right-hand side of Eq. (11). To find the maximum, it is convenient to proceed to spherical coordinates in a three-dimensional space of variables $\{\mu_j\}$. The maximum is achieved at $\mu_1 = \mu_2 = \mu_3$, i.e., resulting in crystallization with three waves of equal amplitude, $\rho_1 = \rho_2 = \rho_3$, and hence a hexagonal 2D crystal, Fig. 2(g).

2. *Herringbone ordering*

The amplitude of the density wave is not the only possible order parameter responsible for crystallization. Consider the transformation of the order parameter on reflection in the symmetry plane containing the wave vector. The order parameter can either remain unchanged, like the density, or change sign. Examples of the latter type are the xy component of a symmetrical tensor, Fig. 3(a), or a transverse vector, Fig. 3(c). Since all other

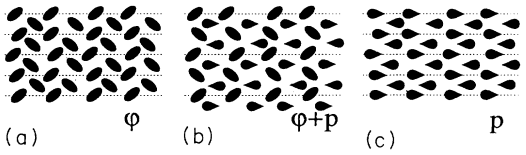

FIG. 3. One-dimensional crystallization with herringbone order (a), antiferroelectric order (c), and a mixed case (b).

symmetry elements transform the wave to other ones, all order parameters can be classified as symmetric or antisymmetric with respect to the reflection. The structures of Figs. 3(a) and 3(c) are equivalent and, moreover, always accompany each other, as shown in Fig. 3(b). One can see from Fig. 3 that the density is also periodic for these structures. However, in contrast to the crystallization mediated by the density waves considered in the previous section, the density here is induced by the primary wave and its amplitude is proportional to the square of the order parameter (see Sec. II C).

Sixfold rotation produces six wave vector $\boldsymbol{k}_j$, in exactly the same way as in the previous section, and the complex amplitudes of the waves ϕ_j form a six-component order parameter. Since the sum $\sum_j \phi_j \exp(i\boldsymbol{k}_j \cdot \boldsymbol{r})$ represents a real quantity, one has $\phi_{j+3} = \phi_j^*$ and, similarly to Eq. (8),

$$\phi_1 = \varphi_1 e^{i\delta_1},\ \phi_2 = \varphi_2 e^{i\delta_2},\ \phi_3 = \varphi_3 e^{i\delta_3},$$
$$\phi_4 = \varphi_1 e^{-i\delta_1}, \phi_5 = \varphi_2 e^{-i\delta_2}, \phi_6 = \varphi_3 e^{-i\delta_3}. \quad (12)$$

The free energy expansion over the powers of φ_j does not contain a third-order term since it changes sign on reflection. Then one has, instead of Eq. (10),

$$\Phi_\varphi = F\varphi^2 + G_1\varphi^4 + G_2(\varphi_1^4 + \varphi_2^4 + \varphi_3^4), \quad (13)$$

where $\varphi^2 = \varphi_1^2 + \varphi_2^2 + \varphi_3^2$. If φ^2 is kept fixed, the minimum of (13) with respect to the components φ_j depends on the sign of G_2. For $G_2 > 0$ one has $\varphi_1 = \varphi_2 = \varphi_3$. The ordered phase is a 2D hexagonal crystal with two molecules per unit cell, Fig. 2(h). This phase is chiral (see Sec. II C).

When $G_2 < 0$, the hexagonal symmetry is broken: $\varphi_1 = \varphi$, and $\varphi_2 = \varphi_3 = 0$, meaning that crystallization occurs only in one dimension. The ordered phase consists of equidistantly spaced rows of the molecules, with the order parameter alternating from one row to the next. Within a row, the molecules possess liquidlike order. The order parameter φ describes either antiferroelectric ordering of transverse vectors of the molecules, Fig. 2(c), or alternating orientations of the 2D nematic director, Fig. 2(a). The latter case corresponds to the herringbone order commonly encountered in ordered smectic liquid crystals [21] as well as in 3D packings of aliphatic chain derivatives [22]. It is illustrated in Figs. 2(e) and 2(f) for crystallization directions parallel and normal to the bond direction. The dashed lines indicate periodicity, and the order within the crystalline rows is liquidlike.

The phases shown in Figs. 2(e) and 2(f) give rise to different low-order diffraction peaks. In Fig. 2(e), the bonds do not lie in the crystalline rows. This gives broad first-order diffraction peaks, reflecting the liquidlike order. In

contrast, the diffraction pattern of the phase shown in Fig. 2(f) shows one narrow peak due to diffraction from the crystalline rows, while the doubly degenerate peak caused by the short-range translational order within the rows is broad. Comparing these results with the experimental data on the diffraction peak widths, we can attribute Fig. 2(e) to the phases S and L_2' whereas Fig. 2(f) corresponds to the phase L_{2h} possessing considerably different widths of the peaks. Clearly, one crystallization order parameter is inadequate, and it is necessary to deal with order parameters describing the transitions to phases with mutually orthogonal directions of crystallization.

We keep the letter φ for the order parameter of the phase shown in Fig. 2(e). For one crystallization wave ($\varphi_1 = \varphi, \varphi_2 = \varphi_3 = 0$) Eq. (13) reduces to

$$\Phi_\varphi = F\varphi^2 - G\varphi^4 + H\varphi^6, \tag{14}$$

where $G = -(G_1 + G_2)$. We take the fourth-order term to be negative, since the transition LS-S is first order. Then the sixth-order term is added to the expansion (14) to ensure the stability of the ordered phase. The term is due to the sum of the invariants

$$H_1\varphi^6 + H_2\varphi^2(\varphi_1^4 + \varphi_2^4 + \varphi_3^4) + H_3\varphi_1^2\varphi_2^2\varphi_3^2,$$

which reduces, for one crystallization wave ($\varphi_1 = \varphi, \varphi_2 = \varphi_3 = 0$), to Eq. (14) with $H = H_1 + H_2 + H_3$. To make the transition LS-S in Langmuir monolayers first order, we take the coefficients F, G, H to be positive. The coefficient F is considered to be temperature dependent whereas G and H are taken to be constant. As F decreases to the value $F_0 = G^2/4H$, a first-order transition occurs from $\varphi = 0$ to $\varphi = \varphi_0$ with $\varphi_0^2 = G/2H$. The transition from the hexatic phase to the phase shown in Fig. 2(f) is described by the order parameter ψ possessing the same symmetry and the same free energy expansion,

$$\Phi_\psi = F'\psi^2 - G'\psi^4 + H'\psi^6. \tag{15}$$

Accordingly, the first-order transition at $F_0' = G'^2/4H'$ gives $\psi_0^2 = G'/2H'$.

To analyze the relationship between the waves shown in Fig. 3 in more detail, let us introduce, in addition to the order parameter φ for the wave of herringbone order of Fig. 2(a), the order parameter P_j — the amplitude of a transverse vector (which can be referred to as polarization). The sixfold rotation C_6 generates six waves with the wave vectors $\boldsymbol{k}_{j+1} = C_6\boldsymbol{k}_j$ and amplitudes $P_{j+1} = C_6P_j$. The twofold rotation $C_2 = (C_6)^3$ changes the signs of both wave vector and polarization vector. Then the requirement that total polarization $\sum_j P_j \exp(i\boldsymbol{k}_j \cdot \boldsymbol{r})$ is a real quantity gives $P_{j+3} = -P_j^*$. The coupling between the waves of the herringbone order parameter ϕ_j and the polarization P_j with equal wave vectors is due to the bilinear combination

$$(\phi_1P_4 + \phi_4P_1) + (\phi_2P_5 + \phi_5P_2) + (\phi_3P_6 + \phi_6P_3) \tag{16}$$

which is invariant with respect to symmetry of the hexatic phase. For one crystallization wave ($\varphi_1 = \varphi, \varphi_2 = \varphi_3 = 0$) Eq. (16) reduces to

$$p\varphi\sin(\delta - \omega), \tag{17}$$

where $P_1 = p\exp(i\omega)$. The contribution of the invariant (17) to the free energy is minimum at $\omega = \delta \pm \frac{\pi}{2}$, i.e., the wave of polarization is shifted to $\frac{1}{4}$ of the period with respect to the wave of herringbone order, as shown in Fig. 3(b). Since the invariant is bilinear, the two order parameters are equally critical to the transition. Minimizing Eq. (17) together with the quadratic terms φ^2 and p^2 in the free energy expansion, one finds a linear combination of φ and p which is the actual order parameter in the presence of both waves.

C. Coupling of the order parameters

Consider the coupling of the crystallization order parameter ϕ with the order parameters η and ξ describing the collective tilt of the molecules and the distortion of the unit cell, respectively. The invariant term should be at least second order over ϕ, to ensure the condition $\sum_j \boldsymbol{k}_j = \boldsymbol{0}$. Recalling that sixfold rotation transforms $\alpha \to \alpha + 2\pi/3$, one constructs the invariant

$$\Phi_{\varphi\xi} = -U[\phi_1\phi_4\xi\cos\alpha + \phi_2\phi_5\xi\cos(\alpha + 2\pi/3) + \phi_3\phi_6\xi\cos(\alpha + 4\pi/3)], \tag{18}$$

where the negative sign of the whole expression is chosen to be convenient for further calculations. For three equal crystallization waves $\varphi_1 = \varphi_2 = \varphi_3$ one has $\Phi_{\varphi\xi} = 0$, since the hexagonal symmetry is not perturbed. For one crystallization wave $\varphi_1 = \varphi$, $\varphi_2 = \varphi_3 = 0$ one arrives at

$$\Phi_{\varphi\xi} = -U\varphi^2\xi\cos\alpha. \tag{19}$$

Taking into account the term $C\xi^2$ of Eq. (4) with positive C, one concludes that crystallization induces distortions $\xi = (U/2C)\varphi^2$. With $U > 0$ one has $\alpha = 0$, i.e., stretching to nearest neighbors, as observed experimentally in phase S.

Coupling with the tilt order parameter η is described by a similar anisotropic invariant,

$$\Phi_{\varphi\eta} = J[\phi_1\phi_4\eta^2\cos 2\beta + \phi_2\phi_5\eta^2\cos(2\beta + 2\pi/3) + \phi_3\phi_6\eta^2\cos(2\beta + 4\pi/3)]. \tag{20}$$

There exists also the product of invariants $I\varphi^2\eta^2$ which is of the same order as Eq. (20). For one crystallization wave, the final expression is

$$\Phi_{\varphi\eta} = I\varphi^2\eta^2 + J\varphi^2\eta^2\cos 2\beta. \tag{21}$$

The anisotropic term of Eq. (21) becomes essential at the tilting transition in the phase $\varphi \neq 0$: it has lower order than the anisotropic terms in the expansion (2) over the powers of η and determines the tilt direction. For $J > 0$ one has $\beta = \pi/2$, i.e., NNN tilt, as is observed at the S-L_2' transition in fatty acids.

Phase transitions in fatty alcohols [18] can be explained with the same signs of the coefficients in the free energy

expansion if one only takes negative D in Eq. (2) for the LS-L_2 transition [23]. In this case the tilting transition from the LS phase causes NNN tilt ($\beta = \pi/2$). The coupling (5) with $V > 0$ gives $\alpha = \pi$, i.e., the unit cell stretches in the tilt direction, as is observed. The term (19) with $U > 0$ causes the unit cell to stretch in the NN direction at the LS-S transition, in accordance with experiment. The tilt direction for the transition from the S phase is governed by the coupling (21), giving NNN tilt for $J > 0$. Thus the difference in behavior of the monolayers of fatty acids and alcohols is explained merely by the opposite sign of D. In the same way as for the fatty acids, the present theory subdivides the tilted phase of fatty alcohols into two phases possessing different symmetries, herringbone-ordered and disordered ones.

The couplings of the crystallization order parameter ψ with the tilt η and the distortion ξ are similar to Eqs. (19) and (21), giving

$$\Phi_{\psi\xi} = W\psi^2\xi\cos\alpha, \tag{22}$$

$$\Phi_{\psi\eta} = -I'\psi^2\eta^2 - J'\psi^2\eta^2\cos 2\beta. \tag{23}$$

The signs of the coefficients are chosen to be convenient in further calculations. In particular, for the tilted herringbone-ordered phase ($\psi \neq 0, \eta \neq 0$) one has with $J' > 0$ the tilt azimuth $\beta = 0$, thus describing the NN tilt in the L_{2h} phase.

The periodic wave of herringbone order causes a periodic variation of the density of the molecules, as is clearly seen in Fig. 3, with the period of the density being half of the period of the structure. Thus the herringbone order wave with the wave vector $\boldsymbol{k}$ induces a density wave with the wave vector $2\boldsymbol{k}$. Using the notation of Sec. II B 1 for this density wave, one can derive the coupled invariant

$$\Phi_{\varphi\rho} = M(\phi_1^2u_4 + \phi_2^2u_5 + \phi_3^2u_6 + \phi_4^2u_1 + \phi_5^2u_2 + \phi_6^2u_3). \tag{24}$$

For one crystallization wave ($\varphi_1 = \varphi, \varphi_2 = \varphi_3 = 0$) it reduces to

$$\Phi_{\varphi\rho} = M\varphi^2\rho\cos(2\delta - \gamma), \tag{25}$$

where $\rho \equiv \rho_1$. The free energy is minimized with respect to ρ giving $\rho = (|M|/2P)\varphi^2$ where the first term of Eq. (10) is taken into account. Thus the herringbone crystallization wave always induces a density wave. It is convenient to take the origin at a density maximum, taking $\gamma = 0$. With this convention, if $M < 0$, the minimum of Eq. (25) is at $\delta = 0$, i.e., the maxima of the herringbone order wave and of the density wave coincide, giving rise to the phase of Fig. 3(a). In the opposite case $M > 0$ the maxima of the herringbone order wave fall on minima of the density wave, whereas the wave of polarization, shifted to $\frac{1}{4}$ of the period due to the coupling (17), follows the density wave. The phase of Fig. 3(c) is realized. When M changes sign, higher-order terms are important and the intermediate phase of Fig. 3(b) results.

One can find out from Fig. 2(h) that the hexagonal crystalline phase caused by three waves $\varphi_1 = \varphi_2 = \varphi_3$ is chiral. The chirality χ induced by the crystallization waves is due to the invariant term

$$\chi\varphi_1\varphi_2\varphi_3\cos(\delta_1 + \delta_2 + \delta_3). \tag{26}$$

Its minimization together with the first term of Eq. (6) gives chirality $\chi \sim \varphi_1\varphi_2\varphi_3$ which vanishes if at least one of the amplitudes φ_j is zero. The sense of the chirality depends on the phases δ_j of the crystallization waves.

III. PHASE DIAGRAM OF LANGMUIR MONOLAYERS

The couplings between order parameters listed in Fig. 2 give a large variety of phase diagrams. Our aim is to explain the experimental phase diagram of the monolayers of amphiphilic molecules shown in Fig. 1(a). Its theoretical description involves at least three order parameters: the one governing collective tilt of the molecules and two others describing the sequence of the three high-pressure phases LS-S-CS. Three order parameters η, φ, and ψ provide a suitable set. More complicated descriptions involving four order parameters are discussed in Sec. IV.

Let us collect all essential terms of the free energy expansion over powers of η, φ, and ψ:

$$\begin{aligned}\Phi = {} & A\eta^2 + B\eta^4 - D\eta^6\cos 6\beta + E\eta^{12}\cos 12\beta \\ & + F\varphi^2 - G\varphi^4 + H\varphi^6 + T\varphi^2\psi^2 \\ & + F'\psi^2 - G'\psi^4 + H'\psi^6 \\ & + (I\varphi^2 - I'\psi^2)\eta^2 + (J\varphi^2 - J'\psi^2)\eta^2\cos 2\beta.\end{aligned} \tag{27}$$

Following the experimental phase diagram, Fig. 1(a), the coefficients F and F' governing the herringbone ordering transitions are considered to be temperaturelike variables whereas the coefficient A responsible for the tilting transition is considered to be a surface-pressure-like one. All other coefficients in the free energy expansion (27) are taken to be constants. The second-order phase transition at the line $A = 0$ gives tilted hexatic phases L_2 and Ov, differing in their tilt azimuth β. These phases are separated by a first-order transition at $D = 0$, provided $E < 0$. The condition $B > 0$ means that the tilting transitions are continuous.

The herringbone-ordering transition LS-S is a crystallization transition, with the order parameter φ. At the line $F_0 = G^2/4H$, the symmetry changes from hexatic to that of a 1D crystal. Although the absence of a third-order term in the free energy expansion means that the transition could possibly be continuous, the observed transition is first order, so that $G > 0$. Similarly, the second crystallization transition S-CS over the order parameter ψ is also a 1D crystallization. It occurs at a lower temperature, and its crystallization wave is orthogonal to the first one.

The tilting transition S-L_2' occurs in the herringbone-ordered phase when $\varphi \neq 0$. Here, the order in η of the coupling term $J\varphi^2\eta^2\cos 2\beta$ is lower than that of $D\eta^6\cos 6\beta$, so that the former determines the tilt azimuth. The NNN tilt in the L_2' phase of fatty acids ($\beta = \pi/2$) is obtained when $J > 0$. Similarly, in the L_2'' phase, the tilt is in the direction which minimizes the

coupling term $(J\varphi^2 - J'\psi^2)\eta^2 \cos 2\beta$, since both φ and ψ are nonzero in the CS phase. The observed NN tilt ($\beta = 0$) is realized for $J\varphi^2 < J'\psi^2$.

The fact that φ is nonzero in the S phase also means that the coupling term $J\varphi^2\eta^2 \cos 2\beta$ influences the position of the tilting transition S-L_2'. Taking $\beta = \pi/2$, the relevant η-dependent terms are

$$[A - (J - I)\varphi^2]\eta^2 + B\eta^4. \tag{28}$$

Then the continuous tilting transition occurs on the line $A = (J - I)\varphi^2$. Here φ is close to its value at the transition $\varphi_0 = (G/2H)^{1/2}$ and increases with decreasing temperature. If $J > I$, the line is shifted to a higher surface pressure with respect to the line $A = 0$ of the LS-L_2 transition, remaining almost parallel to it. Analogously, the line of the tilting transition CS-L_2'' is described by the equation $A = (I + J)\varphi^2 - (I' + J')\psi^2$, since both φ and ψ are nonzero in the CS phase and the tilt azimuth $\beta = 0$ as found above. The line is shifted to a lower surface pressure as observed when $(I + J)\varphi^2 < (I' + J')\psi^2$.

The transition over ψ, realized as the S-CS transition when the temperature decreases, can also be forced by increasing tilt angle at higher temperatures. In addition to its minimum at $(\varphi \neq 0, \psi = 0)$, the free energy in the L_2' phase has a second local minimum at $(\varphi = 0, \psi \neq 0)$, since the transition over ψ occurs at slightly lower temperature. As the tilt angle increases, the latter minimum can become deeper. If the order parameter ψ were nonzero, the coupling (23) would give $\beta = 0$ for $J' > 0$ and would reduce F' in Eq. (15) to $\tilde{F}' = F' - (J' + I')\eta^2$. As the tilt angle η increases, $\tilde{F}'$ reaches the value F_0' and the free energy in the local minimum at $(\varphi = 0, \psi \neq 0, \beta = 0)$ becomes negative. Increasing η further makes this minimum deeper than the minimum at $(\varphi \neq 0, \psi = 0, \beta = \pi/2)$. The observed simultaneous change of the tilt direction and the correlation lengths at the swiveling transition L_2'-L_{2h} is thus explained.

Thus, the phase diagram containing eight phases of different symmetry is explained by the coupling of three order parameters. One is responsible for collective tilt of the molecules, and the other two for one-dimensional weak crystallization involving herringbone ordering of the backbone planes. The free energy expansion (27) involves only the lowest-order terms responsible for the transitions. The present treatment is one of the simplest, but is not unique. Other possible variants, involving additional order parameters, are discussed in Sec. IV.

IV. DISCUSSION

The Landau free energy expansion provides a macroscopic description of the phase transitions in monolayers in the mean-field approximation. In this section we compare the present approach with molecular models and fluctuation theories of monolayers. The phases of Langmuir monolayers which are not contained in the phase diagram of Fig. 1 and their possible descriptions in the Landau theory are also considered. Finally, the possibility is explored that the phase diagram of Fig. 1 can also be explained in the framework of the Landau theory using other sets of order parameters.

Molecular models relate features of a transition to an interatomic interaction potential and provide a more detailed description of a particular transition than the Landau theory. Separate models have been proposed for tilting and herringbone-ordering transitions in monolayer systems. The driving force for the tilting transition is the possibility of preserving an equilibrium mean distance between rodlike molecules when the surface area per molecule is increased [41]. The interaction energy of the rodlike molecules, proportional to the length of the molecules, is dominated by the long-range van der Waals attraction between hydrocarbon chains and their short-range repulsion. There exists some distance between the rods where the attraction and the repulsion balance each other. When the distance between heads of the molecules attached to the water surface is increased, the equilibrium distance can be preserved if the molecules tilt, which allows the cross section normal to the long axes of the molecules to remain hexagonal close packed.

The arguments of this extremely simplified scheme remain qualitatively valid when one takes into account the interaction between molecular heads, together with surface and entropy effects. In particular, the energy difference between NN- and NNN-tilted states of the tilted hexatic phase is a surface effect (independent of molecular length). It is expected to be very weak since it contributes only to the sixth-order term in the free energy expansion. Experimentally, the transition L_2-Ov from NN to NNN tilt is too weak to be revealed by isotherm measurements and has been found only recently using microscopic techniques [8,9]. This picture agrees with the results of molecular dynamics simulations for the tilting phase transition [42–44]. It was shown that the cross-sectional area remains constant when the surface area per molecule is increased [42]. The tilt azimuth found in [43] was not well defined for small tilt angles. NNN and NN tilt were found for even and odd members of the homologous series of perfluorinated amphiphiles [44], respectively. The model intermolecular potential employed in [41] leads to the existence of a low-order term depending on the tilt azimuth. It can be concluded that this overestimates the azimuthal anisotropy. Comparison of the phase diagrams for amphiphiles with different chain lengths and different head groups provides experimental data for more detailed analysis [45].

No molecular model of the herringbone-ordering transition has been developed specifically for Langmuir monolayers. However, another monolayer system possessing the same degree of freedom, adsorbed monolayers of N_2 or H_2 molecules, has been considered with appropriate models [46–50]. The molecular interactions were modeled with a potential of the quadrupole-quadrupole type. The mean-field approximation predicts a continuous transition [47,48]. Cluster-variational methods [49] also predict a continuous transition, and renormalization-group arguments suggest that the transition is first order [50]. Computer simulations disagree in their predictions of the transition order. A continuous transition was found in

a recent simulation [51] (a review of earlier simulations can be found in the cited paper). It should be noted that the above molecular models and computer simulations were all developed for molecules on a hexagonal lattice, so that they are only appropriate for phase transitions between hexagonal and herringbone-ordered crystals. The case of translational freedom appropriate for molecules in mesophases was not analyzed.

Thermal fluctuations are well known to play an essential role in 2D systems. In particular, fluctuations destroy the one-dimensional translational order of the phases of Figs. 2(e) and 2(f) for large separations. The coefficients in the free energy expansions can vary considerably on renormalization, probably changing the transition orders. A renormalization-group analysis of the transitions between tilted hexatic phases was performed in [35,36]. In the notation of the present paper, the long-range renormalization of the coefficients D and E in the expansion (2) was described completely. A renormalization analysis of the free energy expansion (13) for the herringbone-ordering transition has not yet been performed. Renormalization analysis of the expansion (27) involving three order parameters seems an extremely complicated problem.

The hexatic phase was first introduced in the theory of dislocation-mediated melting in two dimensions [52] as a 2D crystal translationally disordered by interacting dislocations in thermodynamic equilibrium which preserve the quasi-long-range order of bond orientations. Considering the phase transitions in Langmuir monolayers from the standpoint of the dislocation melting theory, it is necessary to start from the orthorhombic 2D crystalline CS phase. Two types of melting of an anisotropic crystal are possible, depending on the relationship between its elastic moduli, either to a 1D crystal phase ("type-I" melting) or to an anisotropic hexatic phase ("type-II" melting) [53]. The one-dimensional crystalline order arising from type-I melting exists on an intermediate length scale but is destroyed by fluctuations at long range. In this phase only one set of dislocations with Burgers vectors parallel to each other is essential. The crystallization direction is normal to the bonds and the resulting phase is quite similar to the phase of Fig. 2(f) in the Landau theory. However, the other 1D crystal phase of the Landau theory, whose crystallization wave vector lies along the bonds as shown in Fig. 2(e), does not follow from the dislocation melting theory. In addition, type-II melting does not have an analog in the Landau theory, according to which direct transitions between a hexatic phase and a herringbone-ordered crystal are not allowed. The intermediate phase is either the 1D crystal of Figs. 2(e) and 2(f) or the hexagonal crystal of Fig. 2(h). It is worth noting that the phase sequence observed in liquid crystals with decreasing temperature is stacked hexatic (smectic BH) $\rightarrow$ hexagonal crystal (smectic BC) $\rightarrow$ herringbone-ordered crystal (smectic E) [21].

Some phases observed in monolayers of amphiphiles are not contained on the phase diagram of Fig. 1(a). In fatty acid monolayers at very high pH, an orthorhombic phase (called the "X phase") was observed. Its cell aspect ratio (distortion ξ in the notation of the present paper) was quite different from the value of the S phase [16]. The same aspect ratio was reported for fatty acid monolayers deposited on a solid substrate [54,55]. This phase can probably be interpreted as the phase of Fig. 2(b). Thermodynamic and structural data are not complete enough to make a definite conclusion. A hexagonal crystal phase corresponding to the one of Fig. 2(g) was observed for short fatty acid alcohols at the air-water interface [56] and for the surface monolayer of liquid normal alkanes [57]. The relationship of the former phase to the phases of long fatty alcohols [18] and long fatty acids was not investigated. A phase transition line separating the L_2' phase of Fig. 1(a) into two subphases was found by surface pressure-area isotherm measurements in a fatty acid [6]. A similar transition was reported recently for a fatty alcohol [39]. However, diffraction experiments did not reveal a discontinuity in the tilt angle or distortion. Although the experimental data are clearly not sufficient for any definite conclusion, one can speculate that the transition is probably due to ordering of the only remaining molecular degree of freedom, the orientation of the heads of the molecules. Such orientation is described by a vector lying in the surface plane, i.e., by the same type of order parameter as the collective tilt. In that case an isostructural transition within the L_2' phase is possible.

Let us discuss now the choice of the order parameters in the present theory. The high-temperature condensed phase LS is described as the hexatic phase and the low-temperature phase CS as the herringbone-ordered crystal. Although there is no direct experimental evidence for hexatic order in the LS phase, it is commonly identified as hexatic due to its diffraction pattern, which contains only one (triply degenerate) broad peak. The identification of the CS phase as crystalline is based on its resolution-limited diffraction peaks, indicative of a correlation length greater than 160 lattice spacings, while the unit cell parameters coincide with those of the herringbone-ordered phase of bulk paraffins [14].

The Landau theory does not allow a direct transition from a hexatic phase to a herringbone-ordered crystal. The system must pass through either a 1D crystal of Figs. 2(e) and 2(f) or the hexagonal crystal of Fig. 2(g). The observed intermediate phase S possesses two broad diffraction peaks, which rules out both the hexagonal crystal and the phase of Fig. 2(f) with sharp nondegenerate and broad doubly degenerate peaks. The only possibility which can be identified as the S phase is the 1D crystal phase of Fig. 2(e), whose first-order diffraction peaks are expected to be broad, and the order parameter φ is the only one which could possibly explain the LS-S transition. However, there are two order parameters possible for transition S-CS, namely, one-dimensional crystallization in the orthogonal direction over the order parameter ψ, as proposed in the present paper, and crystallization over the density wave ρ. In the latter case crystallization over ρ occurs in the phase already ordered with respect to φ and a herringbone-ordered crystal results instead of the hexagonal crystal which would appear on direct transition over ρ from the hexatic phase. The order parameter ψ was chosen in the present paper because it explains the whole phase diagram of Fig. 1 in

terms of only three order parameters.

Experimental evidence in favor of the order parameter ψ for the L_{2h} phase is the considerable (3–5 times [14]) difference in the widths of the diffraction peaks in that phase, as is expected for the 1D crystal of Fig. 2(f). This means that the L_2 phase must be subdivided into two phases L_{2h} and L_{2d}, herringbone ordered and disordered, respectively. A transition between these phases possessing different symmetries has not yet been found experimentally. Another possible description of the L_2'-L_2 transition is ordering of the backbone planes parallel to each other due to the order parameter ξ. On this interpretation the phases L_{2h} and L_{2d} would possess the same symmetry, since the distortion ξ in the latter phase is induced by tilt. The phase transition line L_{2h}-L_{2d} can terminate at a critical point in that case, thus explaining the absence of the transition line in the experiment. However, a description of the transitions requires higher-order terms in the free energy expansion. In particular, the coupling term (5) between η and ξ requires the same direction of distortions in phases L_{2h} and L_{2d} possessing the same tilt azimuth. In contrast, the unit cell stretches in the tilt direction to the NN in the L_{2d} phase [58] and shrinks in this direction just below the L_2'-L_{2h} transition [14]. One can introduce a higher-order anisotropic invariant $\xi^2\eta^2\cos(2\alpha+2\beta)$ to explain this behavior, but the theoretical analysis becomes much less definite. More detailed experimental data are required to determine unambiguously the order parameters for all transitions. The choice has to be made from the order parameters listed in Fig. 2 where *all* types of ordering of the hexatic phase allowed by the Landau theory are shown. One can expect that the transitions to the hexagonal crystal phase of short-chain-length fatty alcohols and the X phase of long-chain fatty acids described above can also be described with the order parameters of Fig. 2 and couplings between them, when additional thermodynamic and structural data become available.

V. CONCLUSION

Phase transitions between condensed phases of Langmuir monolayers are due to two of the degrees of freedom of long-chain molecules: the change of orientation of their long axes causes tilting phase transitions at decreasing surface pressure and the herringbone ordering of their short axes (backbone planes) gives rise to crystallization phase transitions with decreasing temperature. Crystallization occurs in two stages via intermediate 1D crystal phases. The couplings between the tilt order parameter and the two order parameters responsible for successive crystallization are sufficient to describe the phase diagram of Langmuir monolayers consisting of eight structurally distinct phases. The present theory describes the upright and tilted hexatic phases at high temperatures, the upright 1D herringbone-ordered crystal and two tilted ones differing in their directions of both tilt and crystallization at intermediate temperatures, and the upright and tilted 2D crystals at low temperatures. Some other structures which are possible in Langmuir monolayers can be found in the list, derived in the paper, of all possible ways of ordering of the hexatic phase allowed in the framework of the Landau theory.

ACKNOWLEDGMENTS

Discussions of the experimental data with H. Möhwald and I. Peterson and their encouragement and support are highly appreciated. V.M.K. thanks P. Dutta, D. Nelson, P. Pershan, S. Sinha, and E. Sirota for helpful discussions of the results. Special thanks are due to R. Kenn, P. Dutta, and M. Durbin for discussions of their experimental results. The authors thank the Deutsche Forschungsgemeinschaft (DFG, Germany) for financing their visits to Germany. This work was partially supported by a grant from the Russian Fundamental Research Foundation.

[1] G.C. Nutting and W.D. Harkins, J. Am. Chem. Soc. **61**, 2040 (1939).
[2] S. Ställberg-Stenhagen and E. Stenhagen, Nature **156**, 239 (1945).
[3] E. Stenhagen, in *Determination of Organic Structures by Physical Methods*, edited by E.A. Braude and F.C. Nachod (Academic Press, New York, 1955), Chap. 8.
[4] M. Lundquist, Chem. Scr. **1**, 5 (1971).
[5] M. Lundquist, Chem. Scr. **1**, 197 (1971).
[6] A.M. Bibo, C.M. Knobler, and I.R. Peterson, J. Phys. Chem. **95**, 5591 (1991).
[7] A.M. Bibo and I.R. Peterson, Adv. Mater. **2**, 309 (1990).
[8] G.A. Overbeck and D. Möbius, J. Phys. Chem. **97**, 7999 (1993).
[9] D.K. Schwartz and C.M. Knobler, J. Phys. Chem. **97**, 8849 (1993).
[10] K. Kjaer, J. Als-Nielsen, C.A. Helm, L.A. Laxhuber, and H. Möhwald, Phys. Rev. Lett. **58**, 2224 (1987).
[11] P. Dutta, J.B. Peng, B. Lin, J.B. Ketterson, M. Prakash, P. Georgopoulos, and S. Ehrlich, Phys. Rev. Lett. **58**, 2228 (1987).
[12] K. Kjaer, J. Als-Nielsen, C.A. Helm, P. Tippmann-Krayer, and H. Möhwald, J. Phys. Chem. **93**, 3200 (1989).
[13] B. Lin, M.C. Shih, T.M. Bohanon, G.E. Ice, and P. Dutta, Phys. Rev. Lett. **65**, 191 (1990).
[14] R.M. Kenn, C. Böhm, A.M. Bibo, I.R. Peterson, H. Möhwald, J. Als-Nielsen, and K. Kjaer, J. Phys. Chem. **95**, 2092 (1991).
[15] M.L. Schlossman, D.K. Schwarz, P.S. Pershan, E.H. Kawamoto, G.J. Kellogg, and S. Lee, Phys. Rev. Lett. **66**, 1599 (1991).
[16] M.C. Shih, T.M. Bohanon, J.M. Mikrut, P. Zschack, and P. Dutta, J. Chem. Phys. **96**, 1556 (1992).
[17] M.C. Shih, T.M. Bohanon, J.M. Mikrut, P. Zschack, and P. Dutta, Phys. Rev. A **45**, 5734 (1992).
[18] M.C. Shih, T.M. Bohanon, J.M. Mikrut, P. Zschack, and P. Dutta, J. Chem. Phys. **97**, 4485 (1992).
[19] M. Durbin, A. Malik, R. Ghaskadvi, P. Zschack, and P. Dutta, J. Phys. Chem. **98**, 1753 (1994).
[20] X. Qiu, J. Ruiz-Garcia, K.J. Stine, C.M. Knobler, and J.V. Selinger, Phys. Rev. Lett. **67**, 703 (1991).

[21] P.S. Pershan, *Structure of Liquid Crystal Phases* (World Scientific Publishers, Singapore, 1988).
[22] A.I. Kitaigorodskii, *Organic Chemical Crystallography* (Consultants Bureau, New York, 1961).
[23] V.M. Kaganer and V.L. Indenbom, J. Phys. II (France) **3**, 813 (1993).
[24] D. Jacquemain, F. Leveiller, S.P. Weinbach, M. Lahav, L. Leiserowitz, K. Kjaer, and J. Als-Nielsen, J. Am. Chem. Soc. **113**, 7684 (1991).
[25] F. Leveiller, D. Jacquemain, L. Leiserowitz, K. Kjaer, and J. Als-Nielsen, J. Phys. Chem. **96**, 10 380 (1992).
[26] L.D. Landau, Phys. Z. Sowjetunion **11**, 26 (1937).
[27] L.D. Landau, Phys. Z. Sowjetunion **11**, 545 (1937).
[28] J.-C. Tolédano and P. Tolédano, *The Landau Theory of Phase Transitions* (World Scientific Publishers, Singapore, 1987).
[29] E.I. Kats, V.V. Lebedev, and A.R. Muratov, Phys. Rep. **228**, 91 (1993).
[30] D.R. Nelson and B.I. Halperin, Phys. Rev. B **21**, 5312 (1980).
[31] R. Bruinsma and D.R. Nelson, Phys. Rev. B **23**, 402 (1981).
[32] S.G. Wolf, M. Deutsch, E.M. Landau, M. Lahav, L. Leiserowitz, K. Kjaer, and J. Als-Nielsen, Science **242**, 1286 (1988).
[33] D. Jacquemain, S.G. Wolf, F. Leveiller, F. Frolow, M. Eisenstein, M. Lahav, and L. Leiserowitz, J. Am. Chem. Soc. **114**, 9983 (1992).
[34] A.A. Acero, M. Li, B. Lin, S.A. Rice, M. Goldmann, I.B. Azouz, A. Goudot, and F. Rondelez, J. Chem. Phys. **99**, 7214 (1993).
[35] J.V. Selinger and D.R. Nelson, Phys. Rev. Lett. **61**, 416 (1988).
[36] J.V. Selinger and D.R. Nelson, Phys. Rev. A **39**, 3135 (1989).
[37] P. de Gennes, *The Physics of Liquid Crystals* (Oxford University Press, London, 1974).
[38] L.D. Landau and E.M. Lifshitz, *Statistical Physics* (Pergamon Press, Oxford, 1980), Part I.
[39] G.A. Lawrie and G.T. Barnes, J. Colloid Interface Sci. **162**, 36 (1994).
[40] J.V. Selinger, Z.-G. Wang, R.F. Bruinsma, and C.M. Knobler, Phys. Rev. Lett. **70**, 1139 (1993).
[41] V.M. Kaganer, M.A. Osipov, and I.R. Peterson, J. Chem. Phys. **98**, 3513 (1993).
[42] J.P. Bareman and M.L. Klein, J. Phys. Chem. **94**, 5202 (1990).
[43] S. Karaborni and S. Toxvaerd, J. Chem. Phys. **97**, 5876 (1992).
[44] N. Collazo, S. Shin, and S.A. Rice, J. Chem. Phys. **96**, 4735 (1992).
[45] I.R. Peterson, V. Brzezinski, R.M. Kenn, and R. Steitz, Langmuir **8**, 2995 (1992).
[46] J. Felsteiner, D. Cabib, and Z. Friedman, Phys. Rev. **18**, 1261 (1978).
[47] A.J. Berlinsky and A.B. Harris, Phys. Rev. Lett. **40**, 1579 (1978).
[48] A.B. Harris and A.J. Berlinsky, Can. J. Phys. **57**, 1852 (1979).
[49] E. Chacón and P. Tarazona, Phys. Rev. B **39**, 7111 (1989).
[50] P. Tarazona and E. Chacón, Phys. Rev. B **39**, 7157 (1989).
[51] Z.-X. Cai, Phys. Rev. B **43**, 6163 (1991).
[52] D.R. Nelson and B.I. Halperin, Phys. Rev. B **19**, 2457 (1979).
[53] S. Ostlund and B.I. Halperin, Phys. Rev. B **23**, 335 (1981).
[54] R. Steitz, E.E. Mitchell, and I.R. Peterson, Thin Solid Films **205**, 124 (1991).
[55] M. Engel, H.J. Merle, I.R. Peterson, H. Riegler, and R. Steitz, Ber. Bunsenges. Phys. Chem. **95**, 1514 (1991).
[56] A. Renault, J.F. Legrand, M. Goldmann, and B. Berge, J. Phys. II (France) **3**, 761 (1993).
[57] X.Z. Wu, E.B. Sirota, S.K. Sinha, B.M. Ocko, and M. Deutsch, Phys. Rev. Lett. **70**, 958 (1993).
[58] P. Tippmann-Krayer and H. Möhwald, Langmuir **7**, 2303 (1991).